Fig. 6. Time courses of changes in intensities of μOR-V, βarr2-C, or βarr1-C in BHK cells. **A**: Confocal imaging of the BHK cells expressing μOR-V, GRK2, and βarr2-C or βarr1-C. For calculation, intensities of the areas within the red line (cytosol) were measured. **B**: Changes in intensities before (a) and 5 min (b) and 10 min (c) after stimulation of DAMGO (10 [7] M) in real time. **C**: Intensity ratio of βarr2-C and μOR-V at the indicated points as in (B). **D**: Intensity ratio of βarr1-C and μOR-V at the indicated points as in (B). Intensity ratio were expressed as ratio of the level at "b" or "c"/the level at "a."

It is also known that β-arrestins are involved in the internalization steps (Gainetdinov et al., 2004). Once receptors are phosphorylated by several kinases, βarr-1 or βarr-2 binds to the receptors, followed by internalization of the receptor/β-arrestin complex (Gainetdinov et al., 2004; Luttrell and Lefkowitz, 2002). Previous reports have shown that baclofen failed to recruit βarr-1 or βarr-2 to the plasma membrane (Fairfax et al., 2004; Perroy et al., 2003). In this study, with BHK cells coexpressing $GB_{1a}R$, GB_2R-V, β-arrestins-C, and GRK4, we investigated the mobility of both GB_2R-V and β-arrestins-C on stimulation by baclofen. This agonist was administered at concentrations and durations at which GRK4 translocated to the plasma membranes, formed GB_2R/GRK4 complex, and consequently desensitized the receptor functions. Our results were in accordance with previous studies showing that GABA_BRs were not internalized and β-arrestins were not mobilized on baclofen stimulation, despite their desensitization under those conditions (Fairfax et al., 2004; Perroy et al., 2003). In the clinical therapy, intrathecal baclofen therapy (ITB) is an established treatment for severe spasticity (Slonimski et al., 2004). Tolerance to ITB for treatment of spasticity is produced by desensitization of the GABA_BR (Kanaide et al., 2007; Nielsen et al., 2002). Desensitization of GABA_BR by baclofen was mediated by protein complex formation of GABA_BR with GRK4 or GRK5 (Ando et al., 2011; Kanaide et al., 2007; Perroy et al., 2003). In such

situation, baclofen did not internalize GABA_BR as shown this study, suggesting that GABA_BR internalization process by itself may not be involved in the development of tolerance to ITB by baclofen.

Recent reports have shown that distinct phosphorylation sites on G protein-coupled adrenergic β_2 receptors act as a "barcode" for the differential functions for β-arrestin, including its receptor-internalization profiles (Nobles et al., 2011). The authors indicated that the specific and distinct patterns of receptor phosphorylation by individual GRKs correlate with different β-arrestin functions. They thus proposed that these distinct phosphorylation patterns create a "barcode" that imparts distinct conformations to the recruited β-arrestin, thus regulating its functional activities. Another report has shown that GABA_BR is internalized by N-methyl-D-asparate (NMDA) receptor stimulation (but not GABA_BR activation itself) due to site-specific phosphorylation of the receptor (serine 867 in $GB_{B1}R$) by calmodulin-dependent protein Kinase II (Guetg et al., 2010). In previous studies, including our own, GABA_BR was not phosphorylated by GRK4 or GRK5, even if they induced GABA_BR desensitization (Kanaide et al., 2007; Perroy et al., 2003). Collectively, these results seem to suggest that agonist stimulation caused little or no phosphorylation of GABA_BR. Thus, internalization of the receptor due to mobilization of β-arrestins or complex formation with β-arrestins was not caused by baclofen.
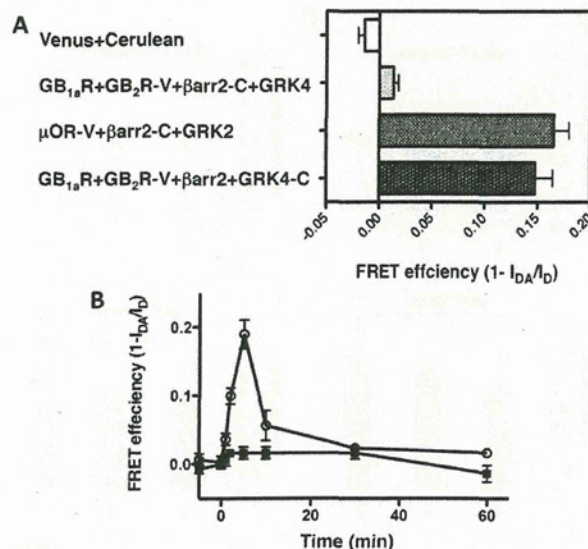
Fig. 7. **A:** Comparison of FRET efficiency on the plasma membranes in BHK cells expressing $GB_{1a}R$, GB_2R-V, and GRK4 with βarr2-C; or μOR-V and GRK2 with βarr2-C on the plasma membranes, with or without stimulation of baclofen or DAMGO for 5 min, respectively. FRET efficiency was calculated from emission spectra. Note the increase of the Cerulean peak emission (488 nm) following photobleaching of Venus (528 nm). I_{DA} = peak of donor emission in the presence of acceptor. I_D = peak of donor emission in the presence of sensitized acceptor. The combination of Venus + Cerulean or $GB_{1a}R$ + GB_2R-V + GRK4-C pairs were used as negative and positive controls for protein–protein interaction, respectively. Each bar represents mean ± SEM of FRET efficiency in independent experiments using six cells with three regions of interest per BHK cell (n = 18). **B:** Changes in the FRET ratio on the plasma membranes in BHK cells coexpressing $GB_{1a}R$, GB_2R-V, and GRK4 with βarr2 and GRK2 with βarr2-C. Photobleaching assay was performed for the periods indicated, and then FRET efficiencies were calculated (n = 3 at each point). The open circles (○) or the closed squares (■) represent data obtained from μOR- or GABA$_B$R-expressing cells, respectively.

On the other hand, some reports with different experimental methods from our own have shown that GABA$_B$R was constitutively (without agonist stimulation) internalized into the cytosol (Grampp et al., 2007). In our study, stimulation by baclofen for up to 90 min failed to cause any detectable, spontaneous internalization, as determined by laser microscopy. However, in our experimental system, we are not aware of the functions of GABA$_B$R. Specifically, we do not know if these receptors elicit acute internalization followed by quick (for example, within 1 min) recycling to the plasma membranes. We were unable to detect basal internalization of GB$_2$R-Venus or recycling of the receptors, as shown by the lack of change in the intensity of GB$_2$R-V at the plasma membranes. Another report, however, has shown that heterodimeric GABA$_B$R internalizes basally and recycles back to plasma membranes (Vargas et al., 2008). The discrepancies between their results and ours are probably due to the different experimental approaches

used. The receptor might internalize to the superficial sites and then recycle quickly to the plasma membrane, and our experimental system may not be able to detect such movements due to the limitation of resolution ability of our laser confocal microscopy.

Further study will be necessary to determine the involvement of β-arrestins in such quick internalization and recycling. Although unknown, it is important to understand their involvement in such short periods of internalization as well as agonist-induced internalization. Such short-term trafficking might play roles in fundamental functions of GABA$_B$R by activating of multifunctioning proteins β-arrestins (Nobles et al., 2011).

In conclusion, these findings suggest that GABA$_B$R fails to undergo agonist-induced and spontaneous internalization in part because of their failure to interact with β-arrestins.

REFERENCES

Agnati LF, Ferré S, Lluis C, Franco R, Fuxe K. 2003. Molecular mechanisms and therapeutical implications of intramembrane receptor/receptor interactions among heptahelical receptors with examples from the striatopallidal GABA neurons. Pharmacol Rev 55:509–550.
Ando Y, Hojo M, Kanaide M, Takada M, Sudo Y, Shiraishi S, Sumikawa K, Uezono Y. 2011. S(+)-ketamine suppresses desensitization of γ-aminobutyric acid type B receptor-mediated signaling by inhibition of the interaction of γ-aminobutyric acid type B receptors with G protein-coupled receptor kinase 4 or 5. Anesthesiology 114:401–411.
Bettler B, Kaupmann K, Mosbacher J, Gassmann M. 2004. Molecular structure and physiological functions of GABA$_B$ receptors. Physiol Rev 84:835–867.
Couve A, Filippov AK, Connolly CN, Bettler B, Brown DA, Moss SJ. 1998. Intracellular retention of recombinant GABA$_B$ receptors. J Biol Chem 273:26361–26367.
Fairfax BP, Pitcher JA, Scott MG, Calver AR, Pangalos MN, Moss SJ, Couve A. 2004. Phosphorylation and chronic agonist treatment atypically modulate GABA$_B$ receptor cell surface stability. J Biol Chem 279:12565–12573.
Gainetdinov RR, Premont RT, Bohn LM, Lefkowitz RJ, Caron MG. 2004. Desensitization of G protein-coupled receptors and neuronal functions. Annu Rev Neurosci 27:107–144.
Galvez T, Duthey B, Kniazeff J, Blahos J, Rovelli G, Bettler B, Prezeau L, Pin JP. 2001. Allosteric interactions between GB$_1$ and GB$_2$ subunits are required for optimal GABA$_B$ receptor function. EMBO J 20:2152–2159.
González-Maeso J, Wise A, Green A, Koenig JA. 2003. Agonist-induced desensitization and endocytosis of heterodimeric GABA$_B$ receptors in CHO-K1 cells. Eur J Pharmacol 481:15–23.
Grampp T, Sauter K, Markovic B, Benke D. 2007. Gamma-aminobutyric acid type B receptors are constitutively internalized via the clathrin-dependent pathway and targeted to lysosomes for degradation. J Biol Chem 282:24157–24165.
Groer CE, Schmid CL, Jaeger AM, Bohn LM. 2011. Agonist-directed interactions with specific β-arrestins determine μ-opioid receptor trafficking, ubiquitination, and dephosphorylation. J Biol Chem 286:31731–31741.
Guetg N, Abdel Aziz S, Holbro N, Turecek R, Rose T, Seddik R, Gassmann M, Moes S, Jenoe P, Oertner TG, Casanova E, Bettler B. 2010. NMDA receptor-dependent GABA$_B$ receptor internalization via CaMKII phosphorylation of serine 867 in GABA$_{B1}$. Proc Natl Acad Sci USA 107:13924–13929.
Kanaide M, Uezono Y, Matsumoto M, Hojo M, Ando Y, Sudo Y, Sumikawa K, Taniyama K. 2007. Desensitization of GABA$_B$ receptor signaling by formation of protein complexes of GABA$_{B2}$ subunit with GRK4 or GRK5. J Cell Physiol 210:237–245.
Kelly E, Bailey CP, Henderson G. 2008. Agonist-selective mechanisms of GPCR desensitization. Br J Pharmacol 153(Suppl 1):S379–S388.
Laffray S, Tan K, Dulluc J, Bouali-Benazzouz R, Calver AR, Nagy F, Landry M. 2007. Dissociation and trafficking of rat GABA$_B$ receptor heterodimer upon chronic capsaicin stimulation. Eur J Neurosci 25:1402–1416.

Luttrell LM, Lefkowitz RJ. 2002. The role of β-arrestins in the termination and transduction of G-protein-coupled receptor signals. J Cell Sci 115(Pt 3):455–465.

Miyawaki A, Tsien RY. 2000. Monitoring protein conformations and interactions by fluorescence resonance energy transfer between mutants of green fluorescent protein. Methods Enzymol 327:472–500.

Nagai T, Ibata K, Park ES, Kubota M, Mikoshiba K, Miyawaki A. 2002. A variant of yellow fluorescent protein with fast and efficient maturation for cell-biological applications. Nat Biotechnol 20:87–90.

Nielsen JF, Hansen HJ, Sunde N, Christensen JJ. 2002. Evidence of tolerance to baclofen in treatment of severe spasticity with intrathecal baclofen. Clin Neurol Neurosurg 104:142–145.

Nobles KN, Xiao K, Ahn S, Shukla AK, Lam CM, Rajagopal S, Strachan RT, Huang TY, Bressler EA, Hara MR, Shenoy SK, Gygi SP, Lefkowitz RJ. 2011. Distinct phosphorylation sites on the β_2-adrenergic receptor establish a barcode that encodes differential functions of β-arrestin. Sci Signal 4:ra51.

Perroy J, Adam L, Qanbar R, Chénier S, Bouvier M. 2003. Phosphorylation-independent desensitization of GABA(B) receptor by GRK4. EMBO J 22:3816–3824.

Riven I, Kalmanzon E, Segev L, Reuveny E. 2003. Conformational rearrangements associated with the gating of the G protein-coupled potassium channel revealed by FRET microscopy. Neuron 38:225–235.

Rizzo MA, Springer GH, Granada B, Piston DW. 2004. An improved cyan fluorescent protein variant useful for FRET. Nat Biotechnol 22:445–449.

Shenoy SK, Lefkowitz RJ. 2011. β-Arrestin-mediated receptor trafficking and signal transduction. Trends Pharmacol Sci 32:521–533.

Slonimski M, Abram SE, Zuniga RE. 2004. Intrathecal baclofen in pain management. Reg Anesth Pain Med 29:269–276.

Terunuma M, Pangalos MN, Moss SJ. 2010. Functional modulation of GABA_B receptors by protein kinases and receptor trafficking. Adv Pharmacol 58:113–122.

Uezono Y, Akihara M, Kaibara M, Kawano C, Shibuya I, Ueda Y, Yanagihara N, Toyohira Y, Yamashita H, Taniyama K, Izumi F. 1998. Activation of inwardly rectifying K⁺ channels by GABA-B receptors expressed in Xenopus oocytes. Neuroreport 9:583–587.

Uezono Y, Kanaide M, Kaibara M, Barzilai R, Dascal N, Sumikawa K, Taniyama K. 2006. Coupling of GABA_B receptor GABA_{B2} subunit to G proteins: Evidence from Xenopus oocyte and baby hamster kidney cell expression system. Am J Physiol Cell Physiol 290:C200–C207.

Vargas KJ, Terunuma M, Tello JA, Pangalos MN, Moss SJ, Couve A. 2008. The availability of surface GABA_B receptors is independent of gamma-aminobutyric acid but controlled by glutamate in central neurons. J Biol Chem 283:24641–24648.

Wilkins ME, Li X, Smart TG. 2008. Tracking cell surface GABA_B receptors using an α-bungarotoxin tag. J Biol Chem 283:34745–34752.

変わる「第二次がん対策推進基本計画」
―第一次がん対策推進基本計画実践後の反省をもとに, がん体験者の視点を取り入れて―

独立行政法人国立がん研究センター研究所がん患者病態生理研究分野分野長
上園　保仁

はじめに

『基礎医学セミナー』を連載で担当させていただいています。2009年12月発行の20巻2号より始まり, これまで5回, 22巻2号まで緩和医療に関する基礎医学がどのように臨床医学につながっているのかについてお話をさせていただきました[1)-5)]。第1回は2007年に施行された「がん対策基本法」における緩和医療関連の基礎医学の立ち位置について, 第2回はがんの痛みをなくすための基礎研究についてその一端をご紹介いたしました。また, 第3回は「がん対策基本法」に基づき計画された「がん対策推進基本計画」(2007〜2012年)がちょうど見直しの時期に来ており, 今後の緩和ケア推進, 緩和ケア研究についてお話をしました。第4回(がん悪液質研究について), 第5回(がんと漢方薬)については, また雑誌を読んでいただければと思います。

厚生労働省の小宮山洋子大臣により行われた「次期がん対策推進基本計画」についての諮問(計画策定についての意見を求めること)について, 2012年3月1日, 基本計画の策定に当たっていたがん対策推進協議会よりその答申がなされました。この「次期がん対策推進基本計画(変更案)」については, 今後国民の意見を聴くパブリックコメントを経て, 5〜6月には閣議決定されるものと思います。

今回は, 「第一次がん対策推進基本計画」とはどのようなもので, 計画はどのように実践され, またその過程でどのような問題があったのか, 平成24年度より施行される「次期がん対策推進基本計画」は第一次計画をベースにどのように改定されたのか, がん体験者の視点からの改定は何か, そして第二次計画において積み残された問題点は何か, についてご紹介できればと思います。

なお, 正確には「次期がん対策推進基本計画(変更案)」[6)]の段階であり, 今後閣議決定を経て「第二次がん対策推進基本計画」となるのですが, 便宜上ここでは「第二次がん対策推進基本計画」として用語を統一させていただきます。

わが国におけるこれまでのがん対策のあゆみ

わが国では, 1981年にこれまでの脳血管疾患に取って代わりがんが死亡原因の第1位となりました。これを機にがん撲滅が国家プロジェクトとなり, 政府は1984年より「対がん10カ年総合戦略」, 1994年より「がん克服新10か年戦略」を策定・実施し, さらに2004年から「第3次対がん10か年総合戦略」を策定し, 現在その施策が行われています。2014年には, 「新たな対がん戦略」と呼ばれる計画も策定に入る段階であると聞いています。厚生労働省としては, 2005年にがん対策全般を総合的に推進するため「がん対策推進本部」を設置し, 同年8月にはがん対策の飛躍的な向上を目的とした「がん対策推進アクションプラン2005」が公表されました(表1)。

このように, 政府, 厚生労働省などががん対策に取り組んでいるものの, 国民の3人に1人はが

表1．わが国におけるがん対策施策のあゆみ

1963年	厚生省がん研究助成金制度の発足
1981年	悪性新生物が死亡原因の第1位となる
1984年	対がん10ヵ年総合戦略の策定(〜平成5(1993)年度)
1994年	がん克服新10か年戦略の策定(〜平成15(2003)年度)
2004年	第3次対がん10か年総合戦略の策定(〜平成25(2013)年度)
2005年5月	がん対策推進本部の設置(厚生労働省)
2005年8月	がん対策推進アクションプラン2005の公表
2006年4月	がん対策推進室の設置(厚生労働省健康局総務課)
2006年6月	がん対策基本法の成立
2007年4月	がん対策基本法の施行
2007年6月	がん対策推進基本計画の策定(閣議決定)
2012年5〜6月	第二次がん対策推進基本計画の策定(閣議決定予定)

(厚生労働省ウェブサイト(http://ganjoho.jp/data/public/statistics/backnumber/
1issao000000068m-att/cancer_control.pdf)より一部改変)

んで死亡し，さらに今後は2人に1人ががんで死亡し，その死亡数も漸増すると推計されるに至り，手厚いがん対策が望まれてきました。そうしたなか，がん患者を中心としてがん対策に関する法律の制定が叫ばれ，2006年6月「がん対策基本法」が成立し，翌年4月に施行されました。さらに，本法律に基づき2007年6月に「がん対策推進基本計画」が策定され，5ヵ年計画として2012年5月まで施行されました。その後は，閣議決定を経て「第二次がん対策推進基本計画」に引き継がれることとなります(表1)。

がん対策基本法の概略

がん対策基本法の骨格についてはすでにご存じのことと思いますが，概略を図1に示します。これはがん対策を総合的に策定し実施するための基本法律であり，①がん予防および早期発見の推進，②がん医療を日本のどこでも同じように受けることができる均てん化の促進，③その他がん研究の促進などを掲げています。また，本法律は国と地方公共団体との密接な関連のもとに協議され，実施されることを求めています。本法律に基

づいて策定されたのが，「(第一次)がん対策推進基本計画」ということです(図2)。これは「がん対策推進協議会」で意見を集約したものが閣議決定され，2007年6月に5ヵ年計画として策定されたものです。

第一次がん対策推進基本計画の概略

図2は，2007年6月〜2012年5月までの5年間で，がん対策基本法に基づいて行うがん対策の総合的指針を掲げたものです。

基本方針および全体目標として，①「がん患者を含めた国民」の視点に立ったがん対策を行うこと，②全体目標達成のために重点的に取り組む課題を具体的に定め，最終的に(1)75歳未満のがん死亡率の20%減少，そして(2)すべてのがん患者およびその家族の苦痛を軽減することと療養生活の質(QOL)の向上をめざすことが定められました。

また，重点的に取り組むべき課題として以下の3課題が取り上げられました。
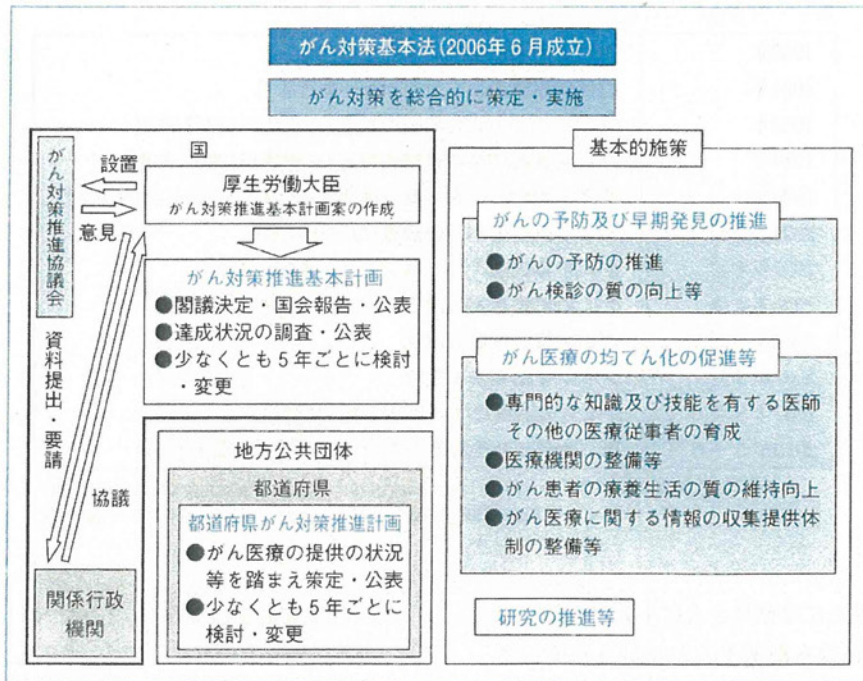①放射線療法及び化学療法の推進並びにこれらを専門的に行う医師等の育成
②治療の初期段階からの緩和ケアの実施

図1．がん対策基本法の概略

（厚生労働省ウェブサイト（http://www.mhlw.go.jp/seisaku/24.html）より）

③がん登録の推進

■ がん対策推進基本計画中間報告書

　2007〜2012年までの5年間の計画の中間点である2010年6月に，がん対策推進基本計画中間報告書が提出されました。基本計画で掲げた大きな2つの全体目標について，その進捗度，また3つの重点課題についての進捗などが報告され，それらの結果に基づいた今後のあり方についての提言が行われました。提言の詳細は第3回の基礎医学セミナーで述べていますが[3]，緩和医療関連の計画に関する内容を簡単に説明すると，全体目標については，

・75歳未満のがん死亡率についてはおおむね順調に減少していること
・がん患者とその家族の苦痛軽減ならびにがん患者のQOL向上については，まずその評価法を

確立しそれに基づき評価を行うべきであること，また目標達成には緩和ケアの推進および医療と介護の連携といった生活支援が重要であること

が挙げられました。

　3つの重点項目のなかで，特に治療の初期段階からの緩和ケアの実施については，個別目標として緩和ケア研修を行うこと，10年以内に緩和ケアの知識・技術を習得した医師を増やすこと，医療用麻薬の消費量の増加を図ることなどが挙げられました。

　その他の重点項目ならびに他の数々の個別案件についても，たとえばがん検診の推進など順当に進んでいない案件に対してほぼその一つひとつに改善点が挙げられました。そして，この中間報告書を参考として「第二次がん対策推進基本計画」を策定することとされました。しかしながら，中間報告書も完全なものではなく，曖昧な点，詰め

1　趣旨

　がん対策推進基本計画は，がん対策基本法に基づき政府が策定するものであり，具体的には，長期的視点に立ちつつ，平成19(2007)年度から平成23(2011)年度までの5年間を対象として，がん対策の総合的かつ計画的な推進を図るため，がん対策の基本的方向について定めるとともに，都道府県がん対策推進計画の基本となるものである。

　今後は，「がん患者を含めた国民が，がんを知り，がんと向き合い，がんに負けることのない社会」の実現を目指すこととする。

2　基本方針

●「がん患者を含めた国民」の視点に立ったがん対策を実施すること。
●全体目標の達成に向け，重点的に取り組むべき課題を定め，分野別施策を総合的かつ計画的に実施すること。

3　重点的に取り組むべき課題

（1）放射線療法及び化学療法の推進並びにこれらを専門的に行う医師等の育成

　　我が国のがん医療については，手術の水準が世界の中でもトップクラスであるのに対して，相対的に放射線療法及び化学療法の提供体制等が不十分であることから，これらの推進を図り，手術，放射線療法及び化学療法を効果的に組み合わせた集学的治療を実現する。
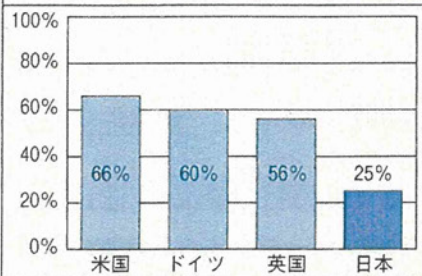
（2）治療の初期段階からの緩和ケアの実施

　　がん患者の多くは，がんと診断された時から身体的な苦痛や精神心理的な苦痛を抱えており，また，その家族も様々な苦痛を抱えていることから，治療の初期段階から緩和ケアが実施されるようにする。
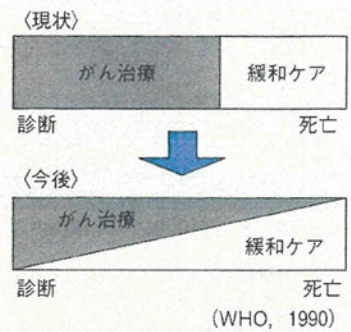
（3）がん登録の推進

　　がん登録は，がん対策の企画立案や評価に際しての基礎となるデータを把握・提供するために必要不可欠なものであるが，我が国では，諸外国と比較してもその整備が遅れていることから，がん登録を円滑に行うための体制を整備する。

がん患者のうち放射線治療(併用も含む)を実施している患者数

出典）第3回がん対策推進協議会における中川恵一委員
　　　（東京大学）からの提出資料をもとに作成

治療の初期段階からの緩和ケアの実施

〈現状〉
がん治療　　緩和ケア
診断　　　　　死亡

〈今後〉
がん治療　　緩和ケア
診断　　　　　死亡
(WHO, 1990)

4　全体目標【10年以内】

●がんによる死亡者の減少(75歳未満の年齢調整死亡率の20%減少)
●すべてのがん患者及びその家族の苦痛の軽減並びに療養生活の質の維持向上

図2．がん対策推進基本計画の概略
　　（厚生労働省ウェブサイト（http://www.mhlw.go.jp/shingi/2007/06/dl/s0615-1b.pdf）より）

きれていない点も多いという指摘もあり，さらに精査して第二次計画を策定すべきであるとの多くの声があがりました。今回の第二次がん対策推進基本計画策定答申の内容は，中間報告書を参考にしつつ，さらに多くのがん体験者の声を取り入れ，策定に至った結果であるといえると思います。こうしてでき上がった「第二次がん対策推進基本計画」を，以下に示します。

■ 第二次がん対策推進基本計画案について

「第二次がん対策推進基本計画」案の概要を，図3に示します。

趣旨は第一次がん対策推進基本計画とほぼ同じですが，加えて第二次計画を策定する根拠が書かれています。第一次計画に比べて第二次計画で内容に変更があったもの，付け加えられたものには下線を引いています。

まず基本方針については，第一次計画では2項目だったのですが，今回新たに原則「全体目標，個別目標を達成するために要する期間の設定」すなわち数値目標がさまざまな個別案件に盛り込まれました。数値目標を設定することは達成がより具体的であり，確実な達成のために重要であり，進化がみられる内容であると思いました。

重点的に取り組むべき課題としては，①放射線

---

1 趣旨

がん対策推進基本計画は，がん対策基本法に基づき政府が策定するものであり，策定，実施された第一次がん対策推進基本計画(平成19～23年度)の結果を踏まえ，基本法第9条第7項規定に基づき前基本計画を見直し，第二次がん対策推進基本計画(平成24～28年度実施)を策定するものである。

今後は，基本計画に基づき「がん患者を含めた国民が，がんを知り，がんと向き合い，がんに負けることのない社会」の実現を目指す。

2 基本方針

①がん患者を含めた国民の視点に立ったがん対策を実施すること
②全体目標の達成に向け，重点的に取り組むべき課題を定めた総合的かつ計画的ながん対策を実施すること
③全体目標を達成するために必要な分野別政策の個別目標を設置し，全体目標，個別目標達成のために要する期間を設定すること

3 重点的に取り組むべき課題

①放射線療法，化学療法，手術療法の更なる充実とこれらを専門的に行う医療従事者の育成
②がんと診断された時からの緩和ケアの推進
③がん登録の推進
④働く世代や小児へのがん対策の充実

4 全体目標【10年のうちの後半5年】

①がんによる死亡者の減少(75歳未満の年齢調整死亡率の20%減少：5年現時点で8.8%)
②全てのがん患者とその家族の苦痛の軽減と療養生活の質の維持向上
③がんになっても安心して暮らせる社会の構築

図3．第二次がん対策推進基本計画案の概要

(厚生労働省ウェブサイト(http://www.mhlw.go.jp/stf/shingi/2r98520000023yyd-att/2r98520000023z2w.pdf)より作成)

療法，化学療法に従事する医師などの育成に加え，手術療法の充実ならびに専門的に行う医療従事者の育成が盛り込まれました。外科を専攻する医師などの減少の危惧から新たに重点化されたものです。また，対象が医療従事者全体へと拡がったのも注目すべきところです。

さらに，②緩和ケアの実施が「治療の初期段階からの」という文言から，よりわかりやすい「がんと診断された時からの」という文言に変わりました。

③がん登録の推進について，第一次計画と同様に重点項目として盛り込まれました。がん登録については，第一次計画でほとんど達成されていなかった項目です。がん登録促進のためのさまざまな工夫，提言も第二次計画には挙げられています（後述）。

新しく重点項目となったものとして，④働く世代のがん患者に対する就労問題などの対策，また第一次計画で抜け落ちていた小児がんに対するがん対策の充実が加わりました。

「全体目標」については，①がんによる死亡者の20％減は第一次計画と同様の目標です。これまでの5年間で8.8％の減少であったので，20％を達成するためには今後の5年で11.2％減少を達成する必要があります。②「全てのがん患者とその家族の苦痛の軽減と療養生活の質の維持向上」については，目標の文言について変化はありません。新たに加わったのが，③「がんになっても安心して暮らせる社会の構築」です。がん体験者の意見・体験をもとに新たに加えられた重要な項目です。

また，第二次計画のなかの「分野別施策と個別目標」についても，第一次計画の反省，加えてがん体験者の視点をもとに，さまざまな個別項目が第一次計画から内容が進化しています。また，第一次計画には盛り込まれていなかった内容についても，前述の「小児がん」をはじめ「医薬品・医療機器の早期開発・承認等に向けた取組」「がん

の教育・普及啓発」「がん患者の就労を含めた社会的な問題」など，さまざまな提言が新たに加わりました。すべてをここで紹介することはできませんが，特にがん患者，がん体験者の視点をもとに盛り込まれた内容について主立ったものを以下に紹介させていただきます。

がん体験者の視点による提言

「第二次がん対策推進基本計画」では，新たに重点的に取り組む課題として「働く世代や小児へのがん対策の充実」，そして全体目標として「がんになっても安心して暮らせる社会の構築」が盛り込まれました。

これは，がん対策推進協議会委員であるがん体験者およびその家族，さらにはアドバイザーとしての多くのがん体験者による，がん対策推進協議会をはじめとしたさまざまな委員会での意見が取り上げられ盛り込まれたものであると思われます。

「働く世代や小児へのがん対策の充実」での，働く世代へのがん対策，特にがん患者の就労問題への対策は，まさにがん体験者の当面している問題です。

がんは，もちろん高齢者に多く発症するものですが，がん患者の30％は働く世代である20～64歳にみられます。今般の手術療法，放射線療法，化学療法の進歩によりがん患者の生存率はかなり上がり，抗がん剤治療を受けながら働いている患者も増えてきています。今回の計画には，特にがん患者やがん体験者の就労について，患者の経済的負担を軽くすることや，働いている企業などにも協力を求め働きながら治療を受けることができる仕組みを作ることなどが盛り込まれました。

多くの数値目標の導入

第二次がん対策推進基本計画には多くの数値目

標が導入され，具体的な結果を求められる計画になっています。

1. 喫煙率の削減

分野別施策と個別目標の「がんの予防」において，喫煙率の抑制についての数値目標が導入されました。10年後（2022年）までに，現状の19.5％の喫煙率を12.2％に引き下げるものです。この数字は，19.5％の喫煙者のうちアンケート調査などでたばこを止めたいと思っている喫煙者の数（約40％）を喫煙ゼロとした場合の数字であるとのことです。喫煙率は第一次がん対策推進基本計画でもたたき台の段階では「半減させる」と盛り込まれる予定であったものが見送られた事実があり，今回はかなり踏み込んだものと考えられます。また，受動喫煙の減少についても数値目標が盛り込まれました。

2. がん検診の受診率の数値目標導入

分野別施策と個別目標の「がんの早期発見」において，がん検診の受診率向上に向けてきめ細かな数値目標が導入されました。第一次がん対策推進基本計画でも数値目標は設定されていたものの，5年の実践のなかでそれは全く数値に届いておらず，非現実的な数値目標といえるものであったという反省からのきめ細かな数値目標の導入です。

・受診率算定の対象を，国際基準にあわせて40〜69歳（子宮頸がんのみ20〜69歳）とする。
・子宮頸がん，乳がんの検診を50％以上とする。
・胃，肺，大腸がんは当面40％をめざす。

一方，がん検診そのものが患者のために本当に有効であるかなどについてもしっかりと議論すべきであるという点も盛り込まれました。

3. がん登録の数値目標

分野別施策と個別目標の「がん登録」において，平成24年度中に47都道府県すべてでがん登録

事業を行うこと，また5年以内にがん患者にがん登録と予後調査を行うなどがん登録の精度を上げること，加えてがん登録の法的位置づけの検討を行うことが盛り込まれました。

おわりに

がん対策を総合的に推進するためには，関係者の連携・協力を進めることのできる体制整備や，都道府県による計画策定を充実させること，またがん対策関係者の意見を集約し把握できる体制を整備すること，さらにがん登録などにおける国民の協力も不可欠です。そのための措置をしっかりと行うことも計画に盛り込まれています。

このように，第一次計画と比べて第二次計画はかなり実践的，そして前衛的なものになっていますが，まだまだ議論が尽くされていない，進め方がはっきりとしていない点も見受けられます。

緩和ケアの質の評価については確たる評価法が定まっていません。たとえば，がんの痛みがどのように取れたかという「除痛率」などを指標として用いるべきであること。

ドラッグ・ラグ問題については，開発者，認可する機関，がん患者などが一同に会して検討しあう場所を設置し包括的に議論すべきであること。

特に適応外薬の問題では，緩和医療での痛み対策に使われる薬剤に適応外薬が多いことから，その解決をめざすべきであること。

などが，がん対策推進協議会委員からも指摘されています。

まだ改善する部分もあるとはいえ，第一次計画からはかなりの進歩，進捗のみられる計画であることは異論のないところです。

第二次がん対策推進基本計画の閣議決定後，同計画に則ってがん対策をしっかりと進めていくことが一番の近道であるので，その対応を見守っていきたいと思います。

追い風となる報告として，以下の記事を紹介し

て本稿を締めくくりたいと思います。

　2012年3月13日，日本医学会，日本癌学会，日本癌治療学会，日本臨床腫瘍学会の4学会より，「がん登録の法制化を！」という要望書が小宮山洋子厚生労働大臣に出されました[7]。がん登録は，第一次，第二次がん対策推進基本計画ともに重点課題として挙げられているものです。平成24年度中には全国47都道府県のすべてで地域がん登録および院内がん登録事業が行われることとなりましたが，各地域での登録の現状には温度差があり，いまだ古いデータを用いているところもあります。がん登録ががんの現状を把握するために必須であるにもかかわらずなかなか普及しないのは，登録情報を今後どのように用いるか，どのようにがん患者にその情報が還元されるのかといった道筋がはっきりしていないことにあると思われます。全国むらなくデータを集め，きめ細かい正確なデータを集めることが最重要であることを鑑み，前述の4団体はがん登録事業を国の事業として位置づけ，100％の登録率をめざすことを提言しています。国によるがん登録事業の法制化が整備されれば，飛躍的に登録事業が進むことが期待されます。

　また，2012年3月16日の厚生労働省プレスリリースによると，4月1日よりこれまでがん対策政策を担当していた健康局総務課設置のがん対策推進室が発展的に拡大され，生活習慣病対策室，地域保健室，保健指導室を再編し「がん対策・健康増進課」になることが決まりました[6]。室から課へと昇格したことで，さらに各室と連携した相互的政策，がん対策が強力に推進できる体制となるであろうと期待されます。

文　献

1）上園保仁：がん対策基本法とがん疼痛基礎医学研究. がん患者と対療 **20**：147-149, 2009
2）上園保仁：がん疼痛基礎医学研究―経験を科学に―. がん患者と対療 **21**：78-81, 2010
3）上園保仁：がん対策推進基本計画に基づく緩和ケア推進・研究の今後. がん患者と対療 **21**：164-169, 2010
4）上園保仁：がん患者の症状緩和のために―がん悪液質の予防，症状改善をめざす基礎医学研究. がん患者と対療 **22**：58-63, 2011
5）上園保仁：がん患者の症状緩和に役立つ漢方薬―漢方薬の有効性を示す，臨床につながる基礎研究―. がん患者と対療 **22**：140-146, 2011
6）厚生労働省ウェブサイト（http://www.mhlw.go.jp/）
7）日本医学会ウェブサイト（http://jams.med.or.jp/）

Short Communication

Inhibition by Pregnenolone Sulphate, a Metabolite of the Neurosteroid Pregnenolone, of Voltage-Gated Sodium Channels Expressed in *Xenopus* Oocytes

Takafumi Horishita[1,*], Susumu Ueno[2], Nobuyuki Yanagihara[3], Yuka Sudo[4], Yasuhito Uezono[4], Dan Okura[1], and Takeyoshi Sata[1]

[1]*Department of Anesthesiology, School of Medicine,* [2]*Department of Occupational Toxicology,*
Institute of Industrial Ecological Sciences, [3]*Department of Pharmacology, School of Medicine,*
University of Occupational and Environmental Health, 1-1 Iseigaoka, Yahatanishiku, Kitakyushu 807-8555, Japan
[4]*Cancer Pathophysiology Division, National Cancer Center Research Institute,*
5-1-1 Tsukiji, Chuou-ku, Tokyo 104-0045, Japan

Abstract. Neurosteroids are known as allosteric modulators of the ligand-gated ion channel superfamily. Voltage-gated sodium channels (Na_v) play an important role in mediating excitotoxic damages. Here we report the effects of neurosteroids on the function of Na_v, using voltage-clamp techniques in *Xenopus* oocytes expressed with the $Na_v 1.2$ α subunit. Pregnenolone sulphate, but not pregnenolone, inhibited sodium currents (I_{Na}) at 3 – 100 μmol/L. The suppression of I_{Na} by pregnenolone sulphate was due to increased inactivation with little change in activation. These findings suggest that pregnenolone sulphate, a metabolite of pregnenolone, suppresses the function of Na_v via increased inactivation, which may contribute to the neuroprotection.

Keywords: pregnenolone sulphate, voltage-gated sodium channel, neuroprotection

Neurosteroids are active steroids synthesized in both the central and peripheral nervous systems, independent of a steroidogenic gland. It is well known that neurosteroids modify the activity of neurotransmitter-gated ion channels and rapidly alter neuronal excitability. Several lines of evidence have shown that these neurosteroids modulate excitotoxicity-mediated neuronal damage through glutamate receptors. For example, pregnenolone and dehydroepiandrosterone (DHEA) protect hippocampal neurons against NMDA-induced neuronal death (1), and pregnenolone sulphate attenuates AMPA-induced inward currents and neurotoxicity in cortical neurons (2). These results suggest neuroprotective effects of neurosteroids and suggest their potential use as a therapeutic medication for brain damage. However, the entire signal transduction cascade of neurosteroids on excitotoxic neuronal injury is still obscure.

Voltage-gated sodium channels play an essential role in action potential initiation and propagation in excitable cells of nerves and muscles (3, 4). Recently, sodium channels are thought to have an important role in excitotoxic damage because sodium channel blockers have neuroprotective effects (5). Here, we examined the effects of neurosteroids on voltage-gated sodium channels using the $Na_v 1.2$ α subunit of sodium channels because it is expressed primarily in the central nervous system, especially the brain. We found that pregnenolone sulphate, but not pregnenolone, inhibited the function of $Na_v 1.2$ expressed in *Xenopus* oocytes.

Adult female *Xenopus laevis* frogs were obtained from Kyudo Co., Ltd. (Saga). Pregnenolone, pregnenolone sulphate, DHEA, and DHEA sulphate were purchased from Sigma-Aldrich (St. Louis, MO, USA). cDNA for rat $Na_v 1.2$ α subunits was a gift from Dr. W.A. Catterall (University of Washington, Seattle, WA, USA), and cDNA for human β_1 subunits was a gift from Dr. A.L. George (Vanderbilt University, Nashville, TN, USA). After linearized cDNA, cRNA were transcribed using T7 ($Na_v 1.2$ α subunits) or T6 (β_1 subunits) RNA polymerase of mMESSAGE mMACHINE kit (Ambion, Austin, TX,

USA). Preparation of *Xenopus laevis* oocytes and micro-injection of the cRNA was performed as described previously (6). $Na_v1.2$ α subunits cRNA was co-injected with β_1 subunits cRNA into oocytes. All electrical recording was performed at room temperature (23°C) using the whole-cell, two-electrode, voltage-clamp technique. The oocytes were perfused at 2 mL/min with Frog Ringer solution containing 115 mmol/L NaCl, 2.5 mmol/L KCl, 10 mmol/L HEPES, and 1.8 mmol/L $CaCl_2$, at pH 7.2. The whole-cell voltage clamp was achieved through these two electrodes using a Warner Instruments model OC-725C (Warner, Hamden, CT, USA). Currents were recorded and analyzed using pCLAMP software (Axon Instruments, Foster City, CA, USA). Neurosteroids were perfused for 2 min to reach equilibrium. All values are presented as the mean ± S.E.M. Data was statistically evaluated by paired *t*-test using GraphPad Prism software (GraphPad Software, Inc., San Diego, CA, USA).

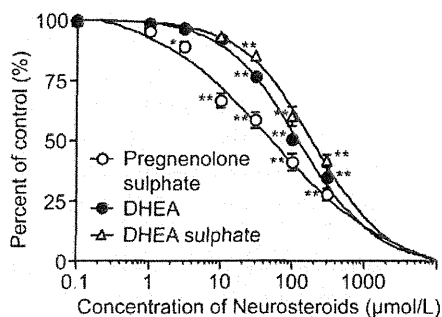First, currents were elicited using a 50-ms depolarizing pulse of −20 mV applied every 10 s from a −90 mV holding potential (causing maximal current, V_{H-90}) or a holding potential causing half-maximal current ($V_{1/2}$) (approximately from −50 to −60 mV) in the absence and presence of neurosteroids. The peak current amplitude in presence of neurosteroids was normalized to that in the control, and the effects of neurosteroids were expressed as percentages of the control. Pregnenolone (100 μmol/L) had little effect on sodium currents (I_{Na}) at both V_{H-90} and $V_{1/2}$ (Fig. 1: A, B, left). Pregnenolone sulphate (100 μmol/L) significantly suppressed I_{Na} to 41% ± 3% of the control at $V_{1/2}$ and to 74% ± 3% at V_{H-90} (Fig. 1: A, B, right). In addition to pregnenolone sulphate, DHEA and DHEA sulphate (100 μmol/L) also reduced I_{Na} to 50% ± 2% and 40% ± 4% at $V_{1/2}$ and to 69% ± 3% and 74% ± 3% at V_{H-90}, respectively (Fig. 1C). Next, we examined the concentration–response relation for inhibition of I_{Na} by neurosteroids at the $V_{1/2}$ (Fig. 2). Pregnenolone sulphate (3 − 300 μmol/L) significantly attenuated I_{Na} in a concentration-dependent manner. The effects of DHEA and DHEA sulphate were 10-fold less potent than that of pregnenolone sulphate. Only ≥ 30 μmol/L of DHEA and DHEA sulphate significantly suppressed I_{Na}. Nonlinear regression analyses of the concentration–response curves yielded the IC_{50} values and Hill slopes of 53 ± 1 and 0.5 ± 0.05 μmol/L for pregnenolone sulphate, 130 ± 8 and 0.8 ± 0.04 μmol/L for DHEA, and 202 ± 6 and 0.9 ± 0.09 μmol/L for DHEA sulphate, respectively.
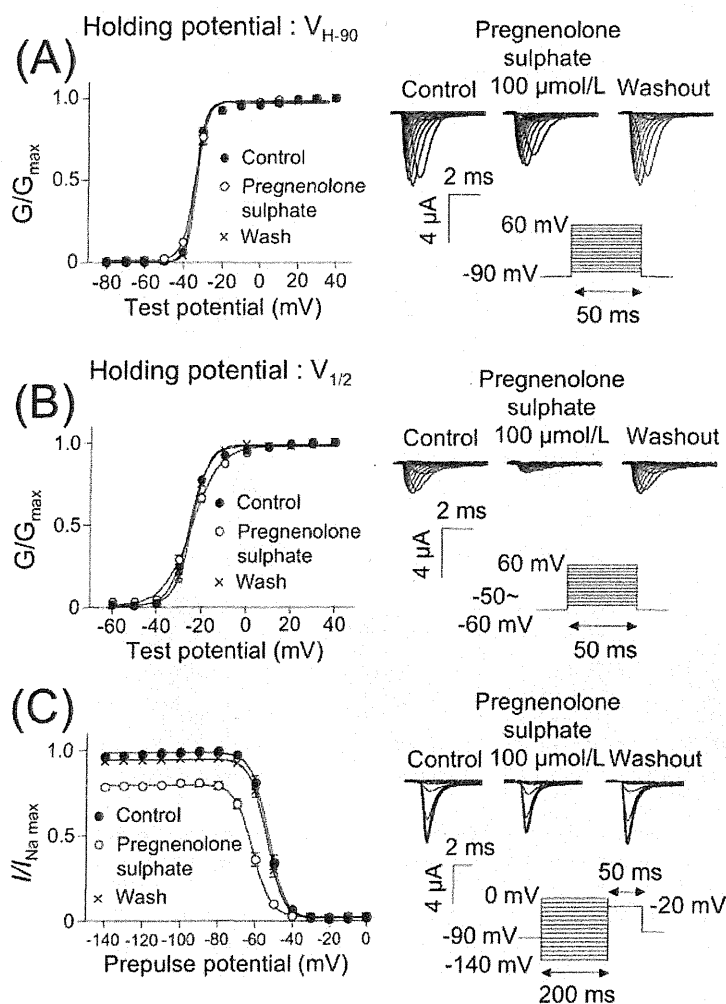
Since pregnenolone sulphate most potently affected
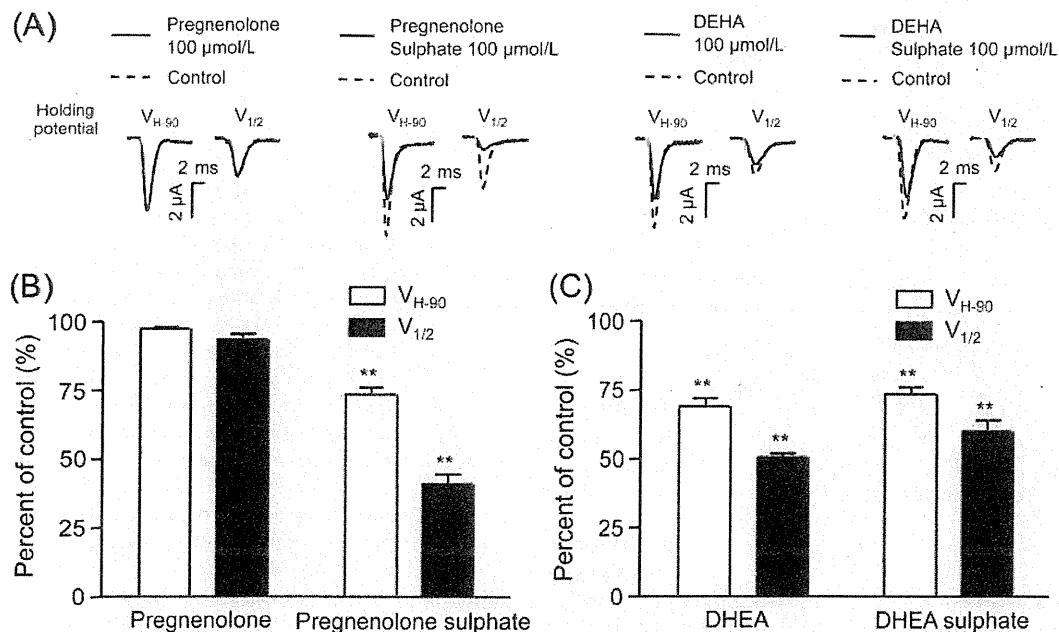
Fig. 1. Effects of pregnenolone, pregnenolone sulphate, DHEA, and DHEA sulphate on sodium currents in *Xenopus* oocytes expressing $Na_v1.2$ α subunits with β_1 subunits. A) Representative traces of sodium currents evoked by 50-ms depolarizing pulses to −20 mV from a V_{H-90} holding potential and $V_{1/2}$ holding potential, in the absence and presence of neurosteroids. Each neurosteroid of at 100 μmol/L was applied for 2 min. B, C) The inhibition of sodium currents by pregnenolone, pregnenolone sulphate, DHEA, and DHEA sulphate. The currents were normalized to the initial values, and percent of the control was calculated. Open columns indicate the effect at V_{H-90}, and closed columns indicate the effect at $V_{1/2}$. Data are represented as means ± S.E.M. (n = 5 − 6). **$P < 0.01$, compared with the control (paired *t*-test).

Fig. 2. Concentration–response curves for pregnenolone sulphate, DHEA, and DHEA sulphate of suppression of sodium currents. Sodium currents were elicited by a 50-ms depolarizing pulse to −20 mV from a $V_{1/2}$ holding potential. Data are represented as means ± S.E.M. (n = 5). The data were fit by the Hill equation to give the IC_{50} values and Hill slopes. IC_{50} values and Hill slopes were calculated by GraphPad Prism. *$P < 0.05$ and **$P < 0.01$ (paired t-test).

the function of $Na_v1.2$, to investigate the inhibitory mechanism of this steroid, we studied the effect of it on sodium current activation and steady-state inactivation. The voltage dependence of activation was determined using 50-ms depolarizing pulses from V_{H-90} and $V_{1/2}$ to 60 mV in 10-mV increments. Normalized activation curves were fitted to a Boltzmann equation (6). The peak I_{Na} was reduced by 100 μmol/L of pregnenolone sulphate at V_{H-90} and $V_{1/2}$ (not shown), but it did not affect the activation curves at V_{H-90} and $V_{1/2}$ (Fig. 3: A, B). Next, currents were elicited by a 50-ms test pulse to −20 mV after 200-ms prepulses ranging from −140 to 0 mV in 10-mV increments from V_{H-90}. Steady-state inactivation curves were fitted to the Boltzmann equation (6). Pregnenolone sulphate shifted the $V_{1/2}$ in the hyperpolarizing direction significantly by 8.2 mV (from −53 ± 1 to −61.3 ± 1 mV) (Fig. 3C). To the best of our knowledge, this is the first direct evidence to demonstrate the inhibitory effect of pregnenolone sulphate on the function of sodium chan-

Fig. 3. Effects of pregnenolone sulphate on activation curves at V_{H-90} holding potential (A) and $V_{1/2}$ holding potential (B) and on inactivation curves (C). Currents were elicited using 50-ms depolarizing steps between −80 and 60 mV in 10-mV increments from a V_{H-90} holding potential (A) and elicited using 50-ms depolarizing steps between −60 and 60 mV in 10-mV increments from a $V_{1/2}$ holding potential (−50 to −60 mV) (B). Pregnenolone sulphate (100 μmol/L) were applied for 2 min. Representative I_{Na} traces from oocytes expressing $Na_v1.2$ with β_1 in the control, presence of 100 μmol/L pregnenolone sulphate, and washout (right panel). Activation curves were fitted to a Boltzmann equation from the I-V curves (left panel). Closed circles represent the control, open circles indicate the effects of pregnenolone sulphate, and crosses indicate washout. Data are shown as the mean ± S.E.M. (n = 5 – 6). C) Currents were elicited using a 50-ms test pulse to −20 mV after 200-ms prepulses ranging from −140 to 0 mV in 10-mV increments from a holding potential of V_{H-90}. Pregnenolone sulphate was applied for 2 min. Representative I_{Na} traces in the control, presence of 100 μmol/L pregnenolone sulphate, and washout (right panel). Inactivation curves were fitted to the Boltzmann equation (left panel). Closed circles represent the control, open circles indicate the effects of pregnenolone sulphate, and crosses indicate washout. Data are shown as the mean ± S.E.M. (n = 5 – 7).

nels of $Na_v1.2$ via increased inactivation.

We found that pregnenolone sulphate, DHEA, and DHEA sulphate, but not pregnenolone, suppressed I_{Na} of $Na_v1.2$ α subunits. Specifically, pregnenolone sulphate had the most potent inhibitory effect among them. Typical plasma concentrations of pregnenolone sulphate have been reported to be 0.2 to 0.4 μmol/L, although those in some healthy subjects have been reported to be approximately 1 μmol/L (7), and normal serum levels of DHEA and DHEA sulphate have been shown to be 10 − 30 nmol/L and 2.0 − 3.0 μmol/L, respectively (8). In some cases and conditions, during pregnancy and in patients with 21-hydroxylase deficiency, however, plasma levels of these neurosteroids can reach micromolar levels (9, 10). The present findings showed that 3 μmol/L pregnenolone sulphate significantly suppressed I_{Na} to 89% ± 2% of the control value. Scholz et al. showed that 10% inhibition of I_{Na} by lidocaine reduced the number of action potentials to 10 from a control response of 21 in 750 ms (11). Therefore, 11% inhibition by 3 μmol/L pregnenolone sulphate would be expected to reduce action potentials. In contrast to pregnenolone sulphate, DHEA and DHEA sulphate suppressed I_{Na} at only high concentrations ($\geq$ 30 μmol/L). In consideration of the above observations, only pregnenolone sulphate would affect neuronal functions through sodium channel inhibition under pathophysiological conditions. In a previous study, pregnenolone as well as pregnenolone sulphate affected the ligand-gated ion channel, GABA$_A$ receptor (12). Therefore, it is interesting to note that only the sulphated steroid of pregnenolone, but not non-sulphated pregnenolone, has an inhibitory effect on sodium channels, suggesting that sulphotransferase and the sulphate moiety of pregnenolone sulphate might play an important role in regulating sodium channel activity. Contrary to pregnenolone and pregnenolone sulphate, both DHEA and DHEA sulphate had similar effects, suggesting that the important moiety in DHEA and DHEA sulphate would be different from that of pregnenolone sulphate.

The present results of channel gating such as activation and inactivation suggest that the enhanced inactivation of sodium channels with little change in activation contributes to the inhibitory mechanism of pregnenolone sulphate. Furthermore, suppression by pregnenolone sulphate at V_{H-90} suggests that it behaves as open channel blockers. This mechanism resembles that of the local anesthetic lidocaine in the point of causing a hyperpolarizing shift in the voltage dependence of steady state inactivation with no effect on that of activation. These results have led us to hypothesize that pregnenolone sulphate and lidocaine, hydrophobic tertiary amine local anesthetics, might share common or overlapping binding sites.

Suppression of voltage-gated sodium channels would be supposed to have a neuroprotective effect because the inhibition of sodium channels leads to suppression of neuronal depolarization, glutamate release, and Na^+ influx, thereby reducing Ca^{2+} influx by means of Ca^{2+} channels, NMDA receptors, and reversal of the Na^+/Ca^{2+} exchanger (13). Pregnenolone sulphate also has effects on the activities of some ion channels, for example, the subtype selective modulation of NMDA receptor (14) and antagonism of the GABA$_A$ receptor and suppression of GABA-induced current (15) at micromolar concentrations. However, it is not clear whether the effects of these modulations of the other receptors can lead to neuronal damage, whereas some new sodium-channel blockers have been shown to have neuroprotective effects (5). Therefore, it gives rise to the possibility that pregnenolone sulphate may be used as a potential neuroprotective medication for the treatment of brain injury. Further in vivo study, however, will be required in the near future.

In conclusion, the present findings demonstrated that pregnenolone sulphate suppresses I_{Na} of $Na_v1.2$ α subunits. These findings would provide a better understanding of the mechanisms underlying the neuroprotective effects exerted by neurosteroids.

Acknowledgments

References

1   Kurata K, Takebayashi M, Morinobu S, Yamawaki S. beta-Estradiol, dehydroepiandrosterone, and dehydroepiandrosterone sulfate protect against N-methyl-D-aspartate-induced neurotoxicity in rat hippocampal neurons by different mechanisms. J Pharmacol Exp Ther. 2004;311:237–245.

2   Shirakawa H, Katsuki H, Kume T, Kaneko S, Akaike A. Pregnenolone sulphate attenuates AMPA cytotoxicity on rat cortical neurons. Eur J Neurosci. 2005;21:2329–2335.

3   Wada A. Roles of voltage-dependent sodium channels in neuronal development, pain, and neurodegeneration. J Pharmacol Sci. 2006;102:253–268.

4   Shin MC, Wakita M, Xie DJ, Yamaga T, Iwata S, Torii Y, et al. Inhibition of membrane Na^+ channels by a type botulinum toxin at femtomolar concentrations in central and peripheral neurons. J Pharmacol Sci. 2012;118:33–42.

5   Carter AJ, Grauert M, Pschorn U, Bechtel WD, Bartmann-Lindholm C, Qu Y, et al. Potent blockade of sodium channels and protection of brain tissue from ischemia by BIII 890 CL. Proc Natl Acad Sci U S A. 2000;97:4944–4949.

6   Horishita T, Harris RA. n-Alcohols inhibit voltage-gated Na^+

channels expressed in *Xenopus* oocytes. J Pharmacol Exp Ther. 2008;326:270–277.

7   Havlikova H, Hill M, Hampl R, Starka L. Sex- and age-related changes in epitestosterone in relation to pregnenolone sulfate and testosterone in normal subjects. J Clin Endocrinol Metab. 2002; 87:2225–2231.

8   Baulieu EE, Thomas G, Legrain S, Lahlou N, Roger M, Debuire B, et al. Dehydroepiandrosterone (DHEA), DHEA sulfate, and aging: contribution of the DHEAge Study to a sociobiomedical issue. Proc Natl Acad Sci U S A. 2000;97:4279–4284.

9   de Peretti E, Forest MG, Loras B, Morel Y, David M, Francois R, et al. Usefulness of plasma prengenolone sulfate in testing pituitary-adrenal function in children. Aca Endocrinol Suppl. 1986; 279:259–263.

10   Hill M, Parizek A, Klak J, Hampl R, Sulcova J, Havlikova H, et al. Neuroactive steroids, their precursors and polar conjugates during parturition and postpartum in maternal and umbilical blood: 3.3beta-hydroxy-5-ene steroids. J Steroid Biochem Mol Biol. 2002;82:241–250.

11   Scholz A, Kuboyama N, Hempelmann G, Vogel W. Complex blockade of TTX-resistant Na^+ currents by lidocaine and bupivacaine reduce firing frequency in DRG neurons. J Neurophysiol. 1998;79:1746–1754.

12   Reddy DS, Kulkami SK. Development of neurosteroid-based novel psychotropic drugs. Prog Med Chem. 2000;37:135–175.

13   Taylor CP, Meldrum BS. Na^+ channels targets for neuroprotective drugs. Trends Pharmacol Sci. 1995;16:309–316.

14   Malayav A, Gibbs TT, Farb DH. Inhibition of the NMDA response by pregnenolone sulphate reveals subtype selective modulation of NMDA receptors by sulphated steroids. Br J Pharmacol. 2002;135:901–909.

15   Majewska MD, Mienville JM, Vicini S. Neurosteroid pregnenolone sulphate antagonizes electrophysiological responses to GABA in neurons. Neurosci Lett. 1988;90:279–284.

Sensation of Abdominal Pain Induced by Peritoneal Carcinomatosis Is Accompanied by Changes in the Expression of Substance P and μ-Opioid Receptors in the Spinal Cord of Mice

Masami Suzuki, Ph.D.,* Minoru Narita, Ph.D.,† Minami Hasegawa, B.S.,‡ Sadayoshi Furuta, Ph.D.,§
Tomoyuki Kawamata, M.D., Ph.D.,‖ Maho Ashikawa, B.S.,‡ Kanako Miyano, Ph.D.,*
Kazuyoshi Yanagihara, Ph.D.,# Fumiko Chiwaki, B.S.,** Takahiro Ochiya, Ph.D.,††
Tsutomu Suzuki, Ph.D.,‡‡ Motohiro Matoba, M.D., Ph.D.,§§ Hiroki Sasaki, Ph.D.,‖‖
Yasuhito Uezono, M.D., Ph.D.##

ABSTRACT

Background: Patients with peritoneal carcinomatosis often report abdominal pain, which is relatively refractory to morphine. It has been considered that a new animal model is required to investigate the mechanism of abdominal pain for the development of optimal treatments for this type of pain.

* Research Resident, ## Chief, Division of Cancer Pathophysiology, ** Research Assistant, ‖‖ Head, Division of Genetics, †† Chief, Division of Molecular and Cellular Medicine, §§ Chief, Department of Palliative Medicine, National Cancer Center Research Institute, Tokyo, Japan. † Professor, Department of Pharmacology; ‡ Student, § Visiting Scientist, ‡‡ Professor, Department of Toxicology, Hoshi University School of Pharmacy and Pharmaceutical Sciences, Tokyo, Japan. ‖ Associate Professor, Department of Anesthesiology & Resuscitology, Shinshu University School of Medicine, Nagano, Japan. # Professor, Laboratory of Molecular Cell Biology, Department of Life Sciences, Yasuda Woman's University Faculty of Pharmacy, Hiroshima, Japan.

What We Already Know about This Topic

- Some patients with cancer have tumor spread throughout the abdominal peritoneum
- The disease of widespread peritoneal tumors, carcinomatosis, can be painful and refractory to conventional analgesic therapies

What This Article Tells Us That Is New

- The investigators developed a mouse model of carcinomatosis
- Behavioral studies indicate pain-related responses are present, and as in patients, the responses are resistant to morphine
- In the future, experimental pain therapies can be studied

Methods: To prepare a peritoneal carcinomatosis model, highly peritoneal-seeding gastric cancer cells, 60As6, were implanted into the abdominal cavity. The nociceptive modality for pain-related behavior was assessed in terms of withdrawal behavior in response to mechanical stimuli and hunching behavior. Tissue samples from mouse dorsal root ganglia and spinal cord were subject to immunohistochemistry and real-time reverse transcription polymerase chain reaction.

Results: Mice with peritoneal dissemination showed significant hypersensitivity of the abdomen to mechanical stimulation and spontaneous visceral pain-related behavior. There was a significant increase in c-Fos–positive cells in the spinal cord in tumor-bearing mice. Those mice exhibited a remarkable increase in substance P-positive neurons in the dorsal root ganglia (control $vs.$ tumor, 15.4 ± 1.1 $vs.$ 24.2 ± 3.6, $P < 0.05$, n = 3). A significant decreases in μ-opioid receptor expression mainly in substance P-positive neurons was observed in tumor-bearing mice (69.3 ± 4.9 $vs.$ 38.7 ± 0.9, $P < 0.05$, n = 3), and a relatively higher dose of morphine was required to significantly reverse the abdominal hypersensitivity.

Conclusion: Both the up-regulation of substance P and down-regulation of μ-opioid receptor seen in the dorsal root ganglia may be, at least in part, responsible for the abdominal pain-like state associated with peritoneal carcinomatosis.

THE moderate or severe pain associated with cancer can impair dramatically the quality of life and the survival of patients and affects 64% of those with metastatic or advanced-stage cancer.[1] The perceived intensity of this pain depends on the specific type of cancer and its location, as well as the each patient's sensitivity to pain.[2] Pain associated with cancer generally is treated with opioids, nonsteroidal antiinflammatory drugs, corticosteroids, local anesthetics, antidepressants, and anticonvulsants, either alone or in combination.[3,4] Despite the availability of these various medicinal treatments, it can be difficult to control pain in some patients with terminal cancer. Accordingly, more effective treatments are needed. Our poor understanding of the mechanism of pain associated with cancers continues to stand as a major obstacle to the discovery of novel analgesics to address this need.

Peritoneal carcinomatosis has been defined as the complex sequence of events by which tumor cells disseminate from their primary organ of origin to establish independent metastatic deposits on the visceral and parietal peritoneal lining of the abdominal cavity. Advanced gastric cancer with peritoneal dissemination is one of the most difficult forms of gastric cancer to treat, and its prognosis remains poor.[5] Patients with peritoneal carcinomatosis report constant, aching abdominal pain. Characteristically, it is poorly localized and is worsened by pressure on the abdomen. Although there have been no rigorous clinical studies, most experts agree that opiate analgesics are relatively ineffective for the treatment of abdominal pain caused by cancerous peritonitis. Compared with somatic pain, which is easily localized and characterized by distinct sensations, visceral pain is diffuse and poorly localized, typically referred to somatic sites, and associated with stronger emotional and autonomic reactions.[6] The abdominal viscera receive dual extrinsic innervation (*e.g.*, spinal and vagal afferents), and accumulating evidence has revealed that there are significant differences in the functions of different nerves innervating the same organ.[6] Adequate stimuli for the production of visceral pain include the distension of hollow organs, traction on the mesentery, ischemia, and endogenous chemicals typically associated with inflammatory processes.[6] Thus, visceral pain differs from somatic pain in several important ways. Several new animal models have been developed for the investigation of cancer pain.[7] The first animal models were developed for the study of primary and metastatic bone tumors,[8] and these were followed by nonbone models of cancer pain that resemble other malignant lesions.[9,10] These animal models were established to enhance our understanding of the neurobiology, pharmacology, and molecular mechanisms of tumor pain.[11–14] However, these are mostly models for somatic pain. The development of

optimal analgesic medications for the treatment of abdominal pain caused by cancerous peritonitis has been hindered by our incomplete understanding of the underlying mechanisms, mainly because of a lack of appropriate animal models to study. In this study, we used 60As6 gastric cancer cells, which are a highly peritoneal-seeding cell line, to develop a novel mouse model of abdominal pain caused by cancer-related peritonitis. Information obtained with this model has provided new insight into the mechanisms that underlie pain caused by cancerous peritonitis and may aid the establishment of potential mechanism-based therapies for treating this pain state.

Materials and Methods

All experiments were conducted in accordance with the ethical guidelines of the International Association for the Study of Pain[15] and were approved by the Committee for Ethics of Animal Experimentation of National Cancer Center (Tsukiji, Tokyo, Japan). In the experiments, efforts were made to minimize the numbers of animals used and their suffering.

Animals
Male C.B17/Icr-scid mice and Institute of Cancer Research mice weighing 22–25 g were used. Mice were purchased from CLEA Japan (Tokyo, Japan) and housed at a room temperature of 23 ± 1°C with a 12-h light–dark cycle. The mice were maintained under specific pathogen-free conditions and provided sterile food, water, and cages.

Cell Lines and Culture
A human scirrhous gastric cancer cell line, HSC60, was established as described previously.[16] The highly peritoneal-seeding cell line, 60As6 was established from HSC60 by orthotopic tissue implantation into scid mice.[17] Briefly, a xenograft tumor of HSC60 cells was transplanted into the gastric wall of a scid mouse. For six iterations, we harvested ascitic tumor cells and performed the orthotopic inoculation of these cells into mice to establish a highly metastatic 60As6 cell line. This cell line was maintained in RPMI1640 medium supplemented with fetal calf serum (10%), 100 U/ml penicillin G sodium, and 100 μg/ml streptomycin sulfate under an atmosphere of 5% carbon dioxide and 95% air at 37°C. To establish transfectants that expressed the luciferase gene, plasmid vectors carrying the firefly luciferase gene, which were called pLuc/Neo, and a transfection reagent, LipofectAMINE 2000 (Invitrogen, Carlsbad, CA), were used as recommended by the manufacturer. Geneticin (500 μg/ml; Invitrogen) was used to select stable transfectants, and transfected clones were screened for luciferase gene expression by detecting bioluminescence using an IVIS system (Xenogen, Alameda, CA). Clones that expressed the luciferase gene were referred to as 60As6Luc cells.

Intraperitoneal Inoculation of 60As6Luc Cells

The density of 60As6Luc cells was adjusted to 1×10^6 cells per 1 ml phosphate-buffered saline (PBS). In the experimental group, the cell suspension was injected into the abdominal cavity through a 26.5-gauge needle inserted into the central abdomen. In the control group, PBS was injected into the abdominal cavity instead of 60As6Luc cells.

Measurement of Tumor Growth Using Luciferase Imaging

For the measurement of tumor growth, whole-body luciferase imaging with an IVIS imaging system was used to visualize 60As6Luc cells under a 10-min integration time for image acquisition, as described previously.[18] Briefly, mice were injected intraperitoneally with 15 mg D-luciferin potassium salt in 1 ml PBS using a 26.5-gauge syringe. They were then kept anesthetized with isoflurane. The relative tumor metastasis burden was determined using Living Image software (version 2.50, Xenogen).

Acute Pancreatitis Model

Caerulein is an analog of cholecystokinin that leads to acute pancreatitis. Acute pancreatitis was induced by repeatedly injecting mice with caerulein (intraperitoneal administration; 50 μg/kg; six times at 1-h intervals).[19,20] Caerulein (Sigma Chemical Co., St. Louis, MO) was dissolved in physiologic saline.

Inflammatory Pain Model

With the mice anesthetized with isoflurane, the plantar surface of the right hind paw was injected with complete Freund's adjuvant (CFA; Mycobacterium tuberculosis; Sigma Chemical Co.) in a volume of 20 μl to create a model of persistent inflammatory pain.[21]

Behavioral Test

Hypersensitivity of the abdomen to mechanical stimulation was quantified by counting the number of withdrawal behaviors (withdrawal of the abdomen away from a von Frey filament, licking of the abdomen as a result of stimulation, or whole-body withdrawal) in response to the application of mechanical stimulation (von Frey filaments with a bending force of 0.02 g) to the abdomen.[19,20] Mice were placed on an increased wire mesh floor and confined under individual overturned black plastic boxes. The von Frey filaments were applied through the mesh floor to different points on the surface of the abdomen. Each filament was applied five times at intervals of 5–10 s, and again after a 1-min rest period for a total of 10 times. Nociceptive behavior was scored as follows: 0 = no response; 1 = immediate slight attempt to escape or light licking or scratching of the stimulated site; 2 = intense withdrawal of the abdomen or jumping. The reported values are the total scores for the responses to 10 challenges. The observer was unaware of the mouse's exper-

imental condition. Behavioral testing was performed on days 14 and 28 after tumor inoculation.

Hunching behavior was examined as described previously with some modifications.[14] Briefly, mice were placed individually in the center of an open field arena and observed for 180 s. The hunching score was the total time (s) the mouse exhibited hunching behavior multiplied by the scoring factor, which was defined according to Sevcik et al.[14]: 0 = normal coat luster, displays exploratory behavior; 1 = mild rounded-back posture, displays slightly reduced exploratory behavior, normal coat luster; 2 = severe rounded-back posture, displays considerably reduced exploratory behavior, piloerection, intermittent abdominal contractions. Behavioral testing was performed on days 14 and 28 after tumor inoculation. The observer was unaware of the mouse's experimental condition. Behavioral testing was performed on days 14 and 28 after tumor inoculation.

In the model of CFA-injected inflammatory pain, hypersensitivity of the paw to mechanical stimulation was quantified by counting the number of paw withdrawals in response to the application of mechanical stimulation (von Frey filaments with a bending force of 0.02 g) to the right paw.[21] von Frey filaments were applied to the plantar surface of the hind paw for 3 s (two applications at an interval of at least 5 s). Paw-withdrawal behavior was scored as defined by Narita et al.[21]: 0 = no response, 1 = a slow and/or slight response to the stimulus, 2 = a quick withdrawal response away from the stimulus without flinching or licking, 3 = an intense withdrawal response away from the stimulus with brisk flinching and/or licking. The final score for each filament was the average of two scores per paw. Morphine hydrochloride (Sankyo, Tokyo, Japan) was dissolved in physiologic saline. Behavioral testing using morphine was performed at day 28 after tumor inoculation in tumor-bearing mice, at 6 h after the last injection of caerulein (50 μg/kg and six times) in the acute pancreatitis model, or at 3 days after the injection of CFA in the inflammatory pain model. In the current study, the analgesic effects of morphine or saline were assessed at 30 min (peak time) after subcutaneous injection by an observer who was blind to the type of treatment. The effects of morphine were assessed in terms of the percentage changes from the basal values (before morphine injection).

Immunohistochemistry

Twenty-eight days after the inoculation of tumor cells, mice were deeply anesthetized with isoflurane and perfused with paraformaldehyde (4%; pH 7.4). The spinal cord and dorsal root ganglia (DRG) were removed rapidly and postfixed in 4% paraformaldehyde for 2 h. Sections of the spinal cord (T10–T11) and DRG (T10–T12) were prepared as described previously.[22] Frozen sections of spinal cords and DRGs were cut at 20 and 10 μm, respectively, using a cryostat (Leica CM1510; Leica Microsystems, Heidelberg, Germany). The sections were blocked in normal horse serum (10%) in 0.01 M PBS for 1 h at room temperature. Each

primary antibody was diluted in 0.01 M PBS containing normal horse serum (10%; 1:5,000 c-Fos; Calbiochem, La Jolla, CA), 1:200 substance P (Neuromics, Edia, MN), 1:250 μ-opioid receptor (MOR; a gift from Masahiko Watanabe, M.D., Ph.D., Hokkaido University Graduate School of Medicine, Sapporo, Japan, October 2010), and anti-MOR antibody against the 1–38 amino acid sequence of the mouse MOR N-terminus[23] and incubated for 1 day at 4°C. They were then rinsed and incubated with each secondary antibody conjugated with Alexa 488 and Rhodamine Red for 2 h at room temperature. The slides were coverslipped with PermaFluor Aqueous mounting medium (Immunon, Pittsburgh, PA), and the fluorescence of immunolabeling was observed by confocal microscopy (LSM510 Meta; Carl Zeiss, Jene, Germany). The anti-MOR antibody used in this study has been shown to be quite specific.[23] The dorsal horn was divided into a superficial layer (L1–2 laminae) and a deep layer (L3–5 laminae), and the number of c-Fos–positive cells was counted in each layer.[24] The cells in 10 randomly selected sections for each marker in each animal were counted, and the average value was determined for each animal. The number of MOR- and substance P-positive profiles in the DRGs was counted as described previously.[25] Briefly, the percentages of MOR- and substance P-positive profiles were determined by counting approximately 2,200 T10–T12 DRG neuronal profiles in tumor-bearing and control mice. We also determined the number of double-positive cells among 500–800 MOR-positive profiles in each mouse. Because we did not use a stereological approach, this quantification may have led to biased estimates of the true numbers of cells and neurons. All counting was performed by an assistant who was blind to the treatment group for the respective sections. To avoid counting neuronal cell bodies twice, for each DRG, we counted sections that were 50 μm apart.

Real-time Reverse Transcription Polymerase Chain Reaction (RT-PCR)

Total RNA was isolated from the thoracic 6–13 th and L1–3 DRG using ISOGEN (Nippon Gene Co., Ltd., Tokyo, Japan) according to the manufacturer's instructions. To obtain first-strand complementary DNA, 5 μg total RNA was incubated in 100 μl buffer containing 10 μM dithiothreitol, 2.5 mM MgCl$_2$, deoxyriboside-triphosphate mixture, 50 units of reverse transcriptase II (Invitrogen) and oligo(dT)12–18 (Invitrogen). Diluted complementary DNA (2 μl) was amplified in a rapid thermal cycler (LightCycler 480; Roche Diagnostics, Mannheim, Germany) in 10 μl LightCycler 480 SYBR Green I Master (Roche Diagnostics) and each oligonucleotide. Primer sequences for the genes of interest (substance P, calcitonin gene-related peptide [CGRP], MOR, and glyceraldehyde-3-phosphate dehydrogenase) are shown in table 1. Size and melting curve analyses were performed to confirm that polymerase chain reaction (PCR) amplicons were specific. To quantify the PCR products, LightCycler 480 quantification software was used to

Table 1. Primer Sequences for the Mouse Genes Characterized in this Experiment

Gene	Primer
GAPDH	Forward primer: 5′ TGTCCGTCGTGG ATCTGAC 3′
	Reverse primer: 5′ CCTGCTTCACCA CCTTCTTG 3′
Substance P	Forward primer: 5′ AAGCCTCAGCAG TTCTTTGG 3′
	Reverse primer: 5′ TCTGGCCATGTC CATAAAGA 3′
CGRP	Forward primer: 5′ TGCAGGACTATA TGCAGATGAAA 3′
	Reverse primer: 5′ GGATCTCTTCTG AGCAGTGACA 3′
MOR	Forward primer: 5′ AGCCCTTCCATG GTCACA 3′
	Reverse primer: 5′ GGTGGCAGTCTT CATTTTGG 3′

CGRP = calcitonin gene-related peptide; GAPDH = glyceraldehyde-3-phosphate dehydrogenase; MOR = μ-opioid receptor.

analyze the exponential phase of amplification and the melting curve, as recommended by the manufacturer. The amount of target messenger RNA (mRNA) in the experimental group relative to that in the control was determined from the resulting fluorescence and threshold values (C_T) using the 2-$\Delta\Delta CT$ method.[26] Each experiment was run twice, and samples were run in duplicate. For each sample, a ΔC_T value was obtained by subtracting the mean C_T value for the control gene (glyceraldehyde-3-phosphate dehydrogenase) from that for the gene of interest (substance P, CGRP, and MOR). The average ΔC_T value for the control group was then subtracted from the value of each animal in the experimental group to obtain $\Delta\Delta C_T$. The fold change relative to the control was then determined by calculating $2^{-\Delta\Delta CT}$ for each sample, and the results are expressed as the group mean fold change ± SD.

Statistical Analysis

All data are presented as the mean ± standard deviation (SD). All the statistical parameters used in the experiments were calculated using GraphPad PRISM (version 5.0a; GraphPad Software, La Jolla, CA). The statistical significance of differences between groups was assessed with one-way ANOVA followed by the Bonferroni multiple comparisons test or unpaired Student t test (two-tailed). A P value of < 0.05 was considered statistically significant.

Results

Characterization of the Peritoneal Metastasis Model

To analyze the progression of peritoneal dissemination of tumor cells, luciferase gene-transfected 60As6 cells were implanted into the abdominal cavities of mice (10^6 cells/cavity). Photon-counting analyses were performed at the site of dis-